Research Article

Dan Luo, Xianglin Pei*, Hai Fu, Xin Yang, Siyu Long, Linyu Zhang, and Wei Gong*

Modification of sodium bicarbonate and its effect on foaming behavior of polypropylene

Abstract: As a potential physical blowing agent, sodium bicarbonate (SB) is environmentally friendly and low in cost, but its low decomposition temperature cannot meet the requirements of polyolefin foam materials. Herein, for enhancing the thermal properties of SB, a modified way was offered to fabricate various SB-based capsules via suspension polymerization. As the modified SB-based capsules, epoxy resin (EP) accompanied with several organic acids was successfully coated on the surface of SB, serving as heat-insulation layer of SB. Various physicochemical characterizations provided reliable evidences for the good coating effect, and the thermal performance of the modified SB was improved. Further, the composite SB capsules were applied for the foaming of polypropylene (PP), and the foaming behavior of the SB-based capsules in PP was significantly improved, with more uniform distribution, smaller cell diameter, and higher cell density. In all, this work fully proved that the coated shells enhanced the thermal properties of SB, and the modified SB capsules significantly improved the foaming quality of foamed PP.

Keywords: sodium bicarbonate, epoxy resin, thermal properties, polypropylene, foaming behavior

* **Corresponding author: Xianglin Pei,** School of Materials and Architectural Engineering, Guizhou Normal University, Guiyang 550025, China; Guizhou Functional Polymer Materials Science and Technology Innovation Talent Team, Guiyang 550025, China, e-mail: xianglinpei@163.com
* **Corresponding author: Wei Gong,** School of Materials and Architectural Engineering, Guizhou Normal University, Guiyang 550025, China; Guizhou Functional Polymer Materials Science and Technology Innovation Talent Team, Guiyang 550025, China, e-mail: gongw@gznu.edu.cn
Dan Luo, Hai Fu: School of Materials and Architectural Engineering, Guizhou Normal University, Guiyang 550025, China; Guizhou Functional Polymer Materials Science and Technology Innovation Talent Team, Guiyang 550025, China
Xin Yang, Siyu Long, Linyu Zhang: School of Materials and Architectural Engineering, Guizhou Normal University, Guiyang 550025, China

1 Introduction

In recent years, facing the increasing demand for foaming agents in the plastic industry, such as polyisocyanurate-polyurethane (PIR-PUR) foams for insulations constructions in wall panel (1) and application of polyurethane foams (RPUF) in flame retardant (2), and environmental problems caused by the reduction of natural resources or the increase of organic waste gas emissions, higher requirements are put forward for the selection and use of foaming agent. The foaming agent is a significant component in the synthesis of foaming materials, such as the commonly used foaming agent of azodicarbonamide (AC) and sodium bicarbonate (3). AC foaming agent could generate a large amount of gas, making it widely used in diversiform applications (4,5). But AC produces a lot of unpleasant nitrogen-containing compounds during foaming process, as well some toxic residue, which would pollute the environment. As a contrast, SB has the advantages of large gas generation and is cheap, easy to obtain, and environment-friendly (6). At the same time, the gas produced by SB decomposition is accessible to dissolve and diffuse in the polymer matrix, which has attracted wide attention to the fields of foaming materials due to its advantageous properties. But bottlenecks have emerged, the low decomposition temperature and wide decomposition temperature range of sodium bicarbonate could lead to the plasticizing effect of foam in polymer (7), which further limit its applications in the foaming area. Therefore, the research to improve the thermal performance of SB is the key problem to solve its engineering application.

In terms of improving thermal properties of SB, some researchers have proved that the thermal properties of SB could be effectively improved by increasing the shell on the surface of SB. Yao et al. (7) also reported a modified SB coated with stearic acid (SA) by melting method and found that the thermal properties of SB have been improved from 112.6°C to 146.9°C. Petchwattana and Covavisaruch (8) reported a SB modified with citric acid (CA) by method of high speed mixing; the results showed that the decomposition temperature of the modified SB was

increased to 130°C. This method slightly increased the decomposition temperature of SB, but the distribution of CA on the surface of SB was not uniform. Cao et al. (9) have investigated a modified SB coated with eruca-mides solution and found that the initial decomposition temperature of SB was raised from 115°C to 165.8°C, and the decomposition temperature range narrowed from 61°C to 46.7°C after the modification. Although these methods can increase the decomposition temperature of SB, it is still lower than the melting temperature of PP. PP is one of the most important general-purpose plastics with excellent mechanical properties, high-heat resistance, and excellent characteristics and is nontoxic, cheap, and has been widely used in automobiles, home appliances, construction, and other fields (10–12). Based on these considerations, it is of great significance to explore new modification methods and to improve the decomposition temperature of SB and its application as a foaming agent of polyolefin materials.

Epoxy resin is a kind of macromolecular thermo-setting polymer with good viscosity, thermal stability, and mechanical strength accompanied, so it is widely used in various industrial fields such as adhesives and paints (13,14). In this paper, to improve the thermal properties of SB, epoxy resin with several organic acids was coated on the surface of SB. The effect of surface modification of SB by EP and different organic acids on its thermal properties was systematically investigated, and the synthesized SB-based capsules were applied to the foaming of PP, and the foaming behavior of modified SB was further explored. This study not only conforms to the concept of environmentally friendly materials, but also provides direction guidance for the development of PP foaming products.

2 Experimental

2.1 Materials

Diglycidyl ether of bisphenol-A (epoxy value = 0.51 mol/100 g) epoxy resin and hardener of triethylenetetramine (TETA) were procured from the Hindustan Ciba Giegy Ltd and DMP-30 (2,4,6-tris(dimethy-laminomethyl)phenol) used as curing aids were supplied by Shanghai Resin Company, China. Absolute ethanol and sodium bicarbonate (AR) were obtained by Tianjin Damao Chemical Reagent Company. Sodium dodecyl sulfonate (SDBS), SA, palmitic acid (PA), and CA were purchased from Aladdin. Polypropylene (PP, T-30) and low-density polyethylene (LDPE)

were produced by Petro-China Co., Ltd. Nanometer organic montmorillonite (OMMT) was procured from Zhejiang Fenghong New Material Co., Ltd.

2.2 Synthesis of the various SB-based capsules

Firstly, SB was grinded with a ball mill and selected to collect the size fraction below 400 meshes. 1 g of EP was dissolved in 120 mL of ethyl alcohol and ultrasound around 5 min to obtain homogeneous mixture. The mixture of EP was placed in a 250 mL three-necked flask equipped with a magnetic stirrer; the flask was placed in an oil bath. Sodium bicarbonate (5 g) was added into the above solution and stirred for 20 min at room temperature. Subsequently, curing agent of TETA (10% mass fraction relative to EP), dispersing agent of SDBS, and catalytic agent of DMP-30 were dispersed in the above liquid and maintained to allow for 40 min at 40°C in an oil bath. The mixture was then heated to 70°C and sequentially stirred for 6 h. (It is worth mentioning that the weight loss rate of pure sodium bicarbonate is 3.18% at 70°C for 6 h; therefore, the longer heat treatment time in the preparation process has little effect on the later preparation, as shown in Figure A1). Finally, the obtained composite (EP@SB) was washed with deionized water and ethanol and dried in an oven at 60°C for 48 h for later use.

The CA was mixed in a 250 mL three-necked flask with 120 mL of ethanol, followed by the addition of the nitric acid to adjust the pH to 2. The EP@SB composite was added to the above mixed liquid. The solution was kept stirring for 15 min to obtain homogeneous mixture at room temperature and then heated to 70°C for 7 h. Finally, the reaction was cooled at room temperature, and the obtained composite (CA/EP@SB) was washed three times with ethanol and distilled water to remove impurities and dried in an oven at 60°C for 48 h. Similarly, the experiments were prepared with PA and SA compounds to obtain the samples of PA/EP@SB and SA/EP@SB.

2.3 Preparation of the foamed masterbatch and substrate

Different SB-based capsules were blended with LDPE at a weight ratio of 1:9 in a torque rheometer (XSS-300,

Shanghai Kechuang Rubber & Plastic Machinery Equipment Co., Ltd), and these composites were mixed about 6 min under a temperature of 100°C (SB did not decompose in this process, confirmed as in Figure A2). The above composites were cooled at room temperature and crushed with a pulverizer to acquire different types of foam masterbatches.

The blends of PP with 3 wt% MMT were made by twin-screw extruder (TSE40A, Nanjing Ruiya polymer Equipment Co., Ltd). The melting temperatures of PP/MMT from zone 1 to zone 10 were 170°C, 173°C, 176°C, 180°C, 185°C, 186°C, 187°C, 189°C, 190°C, and 193°C, respectively. Afterwards, the PP/MMT extrudate was cooled in a water bath and cut into small particles, and dried at 80°C for 12 h in a vacuum oven.

2.4 Preparation of the PP foaming materials

PP/MMT mixed with 15 wt% previously prepared masterbatch and SB-based capsules foaming agents were injected using an injection molding machine with feeding zone temperature of 190°C, 189°C, 188°C, and 187°C, respectively, and the injection speed was 95% with injection pressure of 40 MPa. Then, the dumbbell-shaped PP/SB, PP/EP@SB, PP/PA/EP@SB, PP/SA/EP@SB, and PP/CA/EP@SB foaming products were obtained; they were designated by PP-1, PP-2, PP-3, PP-4, and PP-5, respectively.

2.5 Foam characterization

The densities of the PP/MMT blends and the foamed samples were measured by using a water displacement method. The cell size was calculated by SEM, and at least 100 cells were tested to acquire the average cell diameter. Image Proplus software was used to analyze the SEM images and the average diameter and cell density were calculated as follows (14,15):

$$N_0 = \left[\frac{nM^2}{A}\right]^{\frac{3}{2}}\left[\frac{1}{1 - V_f}\right] \tag{1}$$

$$V_f = \frac{\rho - \rho_\mathrm{f}}{\rho} \tag{2}$$

where N_0 was the cells' density per unit volume, ρ and ρ_f were the density of sample before and after foaming, respectively. n was the number of cells observed under microscope and V_f was the porosity percentage. A was the field observed under the microscope, and M is the magnification factor.

2.6 Characterizations

Fourier-Transform Infrared spectroscopy was conducted on a FT-IR, NEXUS670, Thermo Nicolet USA, and the wavelength range was 500–4,000 cm^{-1}. The thermal properties of the SB-based capsules were evaluated by thermogravimetry (TGA, Q50, iversePerkin Elmer, USA), and TGA was conducted from the 40°C to 600°C at 10°C/min under N$_2$ atmosphere. The thermal stability investigation of the modified SB composites was characterized by Differential Scanning Calorimeter (DSC, Q10 Perkin-Elmer, USA); the test temperature was from room temperature to 80°C for 10 min to eliminate the mass error of the sample. Then it was cooled to room temperature and heated to 300°C at a rate of 10°C/min in N$_2$ atmosphere. Nitrogen adsorption instrument measurement was conducted on a TriStar® II 3020, Micromeritics. The morphology of the modified SB composites was measured by SEM (KYKY-EM6200, Beijing Science and Technology Instrument Co., Ltd.). Transmission Electron Microscope (TEM, Tecnai F20, FEI, USA) was used to study the shell thickness of the capsules. Thermal conductivity of the samples was tested by utilizing hotwire thermal conductivity meter (TC3000, Xiaxi Co., Ltd., China) at room temperature.

3 Results and discussion

3.1 Structure of the synthesized sodium bicarbonate capsules

To better understand the structure of the modified SB, a series of characterizations were conducted. As shown in Figure 1, in the FT-IR spectra, the prominent peaks at 835 cm^{-1} and 696 cm^{-1} in SB were assigned to the stretching vibration of CO$_3^{2-}$ (Figure 1b), and the peak at 1,509 cm^{-1} in EP was corresponding to the stretching vibration of benzene ring (16,17). In the pure SA, PA, and CA, the peaks at 2,923 cm^{-1} and 2,849 cm^{-1} were originated from the symmetrical stretching vibration of the C–H of CH$_2$ and CH$_3$ (17,18) (Figure 1c). Moreover, the peak at 1,708 cm^{-1} was ascribed to the stretching of the C=O groups of the several organic acids, and the
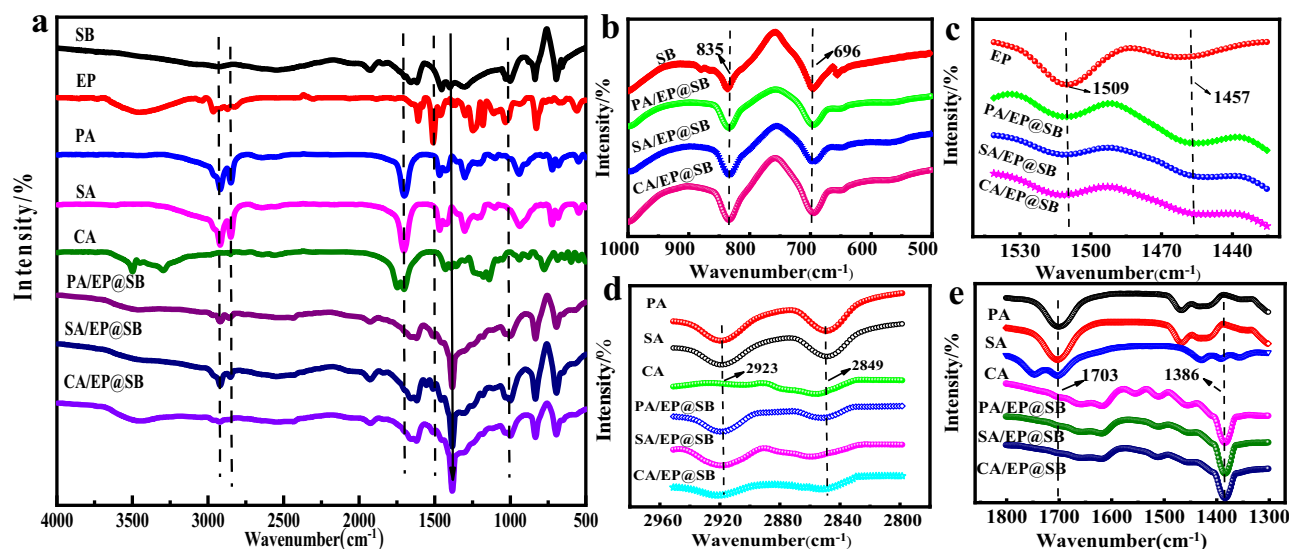
Figure 1: (a) FT-IR spectra of the pure SB, PA, SA, CA, EP, PA/EP@SB, SA/EP@SB, and CA/EP@SB, (b−e) were the locally enlarged graph of graph (a).

broad region of the CA spectrum at the range of 3,290–3,500 cm^{-1} came from the contribution of –OH bonds. After modification, as mentioned above, only absorption peak at 1,703 cm^{-1} was disappeared and others peaks still retained, whereas an obvious peak at 1,386 cm^{-1} corresponding to –COO groups was appeared (19) (Figure 1d), which may appear from the chemical reaction between organic acid and epoxy resin, indicating that the organic acid was grafted on the surface of the epoxy coating. FT-IR spectra indicated that the epoxy resin and organic acids were successfully coated on the surface of SB.

The morphology of the SB-based capsules was observed by SEM, as shown in Figure 2. It could be seen that the pure SB exhibited smooth surface (Figure 2a and a$_1$). After modified with EP, the surface of EP@SB presented a lot of wrinkles without visible agglomeration and exposed SB particles, indicating that the SB was effectively enclosed in EP (Figure 2b and b$_1$). Moreover, the EP@SB was further modified by a series of organic acids that could interact with EP. As shown in Figure 2c−e, the surface of the secondary modified products of PA/EP@SB, SA/EP@SB, and CA/EP@SB became rougher than for EP@SB. This may be due to the hydrogen bond interaction between organic acids and EP, which made the molecular chain of EP become dense, and the intertwined molecular chains made the surface rough (20). These data proved that the EP and some organic acids were successfully attached on the surface of SB, and the rough surface with intertwined molecular chains could

improve the property of heat insulation of the outer shells. Moreover, in order to identify the dispersion of SB-based compounds before and after modification, N$_2$ adsorption isotherms were used. According to the isotherm adsorption curve and Brunauer−Emmet−Teller (BET) equation fitting, the specific surface area of SB, EP@SB, PA/EP@SB, CA/EP@SB, and SA/EP@SB was calculated as 5.82, 6.45, 9.89, 9.32, and 7.78 m^2/g, respectively, as shown in Figure A3, which indicated the good dispersion of SB-based compounds. To further prove the morphology of the modified SB, TEM was conducted. Herein, sample of EP@SB was used as example, as shown in Figure 2b$_1$, the EP@SB showed an irregular shell profile, in which core of SB is more contrast, and shell of EP coating layer is less contrast, demonstrating that EP was successfully coated on the surface of SB. Figure 2c$_1$−e$_1$ displayed an obvious boundary between the core and the shell, and their shell was rougher than observed in Figure 2b$_1$, which also proved that the organic acids were grafted on the EP. These results further suggested that the epoxy resin and organic acids were successfully coated on the surface of sodium bicarbonate.

3.2 Thermal properties of the synthesized SB-based capsules

The influences of epoxy resin and organic acids coating on the thermal behavior of SB were characterized by TG.
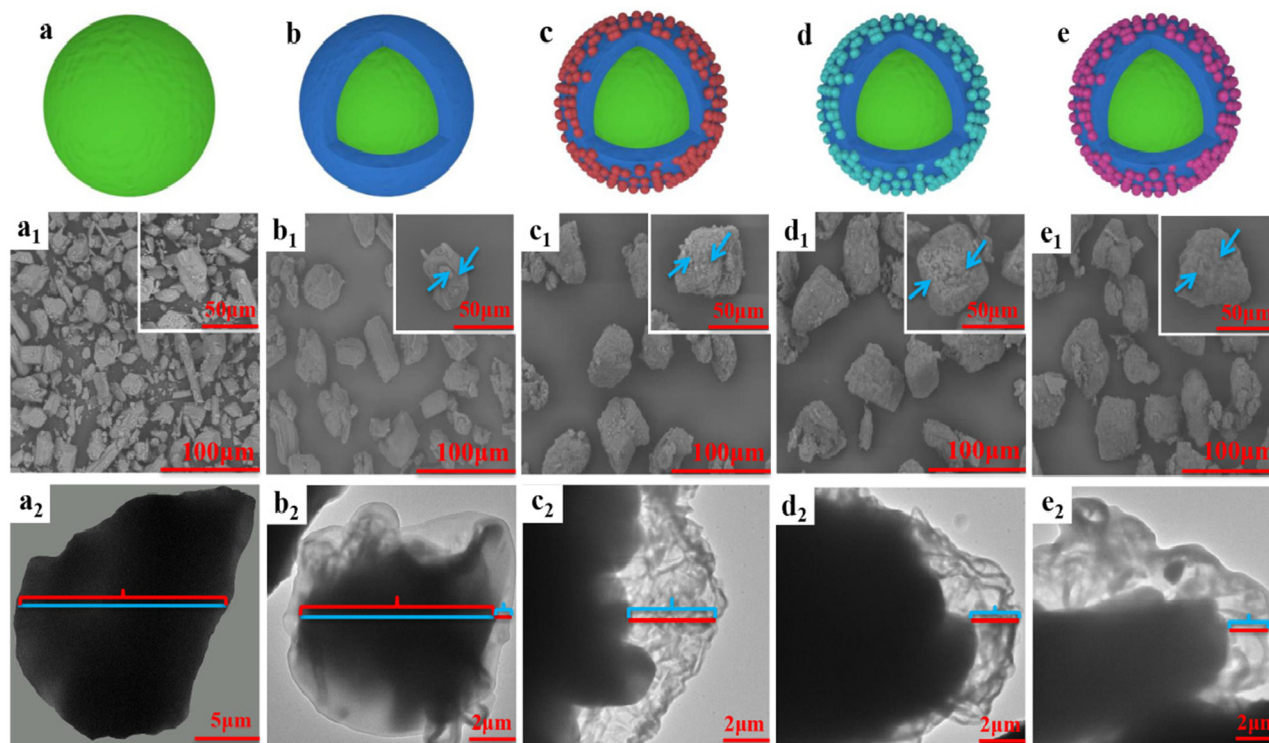
Figure 2: SEM and TEM images of the SB with coating layers. (a) SB, (b) EP@SB, (c) PA/EP@SB, (d) SA/EP@SB, (e) CA/EP@SB.

As shown in Figure 3a and Table 1, the initial decomposition temperature (T_0) of the pure SB was 119°C, with 63% residue at 600°C. In the curve of EP@SB, the thermal behavior of weight loss was obtained in the temperature range of 150–200°C and 250–600°C. Among them, the first broad temperature range was owed to the decomposition of SB, while the second wide temperature range was due to the partial and complete decomposition of epoxy resin. It could be seen that the initial decomposition temperature of EP@SB was 36°C higher than that of pure SB, which was mainly due to the heat transfer of the outer epoxy resin shell, causing the gradual thermal decomposition of SB (21,22). When the temperature was higher than the decomposition temperature of epoxy, the outer capsule of epoxy resin was swelled until the gas escaped. To further improve the thermal performance of EP@SB, a variety of organic acids were coated on the basis of EP@SB. It could be seen that the T_0 of PA/EP@SB, SA/EP@SB, and CA/EP@SB was 178°C, 174°C, and 165°C, with weight loss of 28%, 24%, and 30%, respectively. The T_0 was increased by nearly 46–59°C compared with pure SB. Therefore, the effect of secondary modification with organic acid was better than that of primary modification with epoxy resin, which may be due to some chemical reaction or interaction between

epoxy resin and organic acids, resulting in the increase of crosslinking structure density in the molecular chain and the difficulty in the movement of macromolecular chain. These results showed that we have successfully enhanced the thermal stability and improved the thermal insulation performance of SB.

The thermal stability of the pure SB, EP@SB, PA/EP@SB, SA/EP@SB, and CA/EP@SB samples was also explored by DSC. It could be observed from Figure 3b and Table 1 that the maximum peak temperature (T_p) of pure SB was 152°C, with a decomposition temperature range (ΔT) of 69°C. After being modified by epoxy resin, the ΔT decreased from 69°C to 46°C compared to pure SB, and the T_p was also increased to 171°C, which was attributed to the increase of SB coating shell, leading to better barrier effect (23). After further coating with some different organic acids, it could be observed in Table 1 that when PA was added, the maximum peak temperature of PA/EP@SB increased from 152°C (pure SB) to 186°C, suggesting better thermal stability, and the decomposition temperature range was 28°C, which was narrower than pure SB sample by 41°C. The results caused by when the heating temperature is more than the decomposition of coating shell, and the coating shell instantaneously are decomposed and ruptured, the temperature of the core of
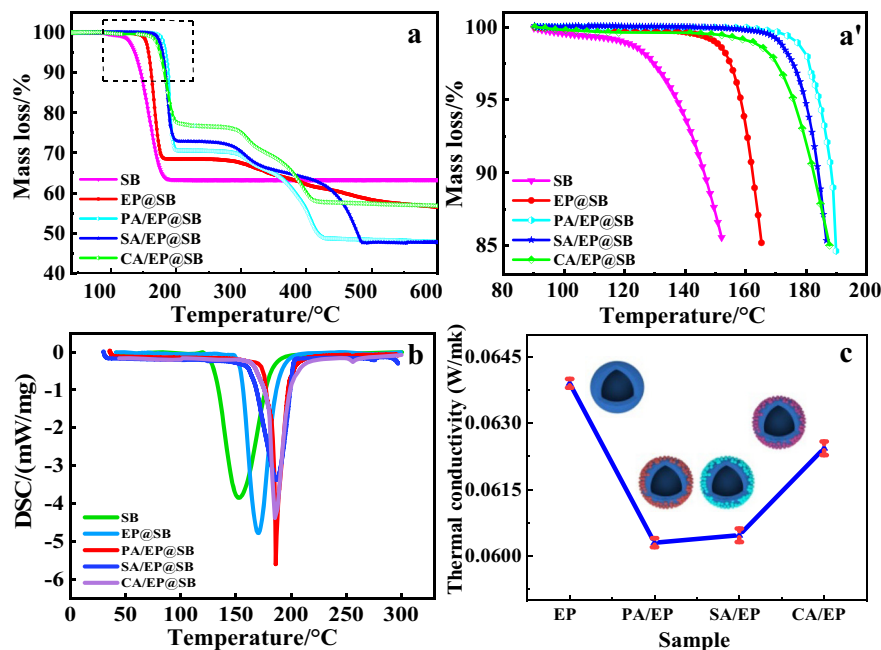
Figure 3: (a and a') TG curves of the SB-based capsules. (b) DSC curves of the SB-based capsules. (c) Thermal conductivity of the EP and PA/EP, SA/EP, and CA/EP.

SB will rise rapidly and the temperature at this time was the maximum endothermic peak of SB. Furthermore, the decomposition temperature range of SA/EP@SB and CA/EP@SB was 31°C and 38°C, and the maximum peak temperature was 186°C and 185°C, respectively. By comparison, the multilayer coating effect of organic acids was better than that of epoxy single-layer coating for SB, especially the modification for PA/EP@SB. These results demonstrated that the decomposition temperature range of SB decreased with different coating layers, and multiple coating layers would give SB better thermal stability.

The improvement of SB-based capsules' thermal performance encouraged us to explore the thermal conductivity of the coating shell, and the thermal conductivity of the pure EP, EP/CA, EP/SA, and EP/PA was measured by Thermal conductivity meter (TC300, Xi'an Xiaxi Electronic

Technology Co., Ltd.). As shown in Figure 3c, the thermal conductivity of pure EP was 0.0639 W/m K at room temperature. After introducing some different organic acids, the thermal conductivity of EP slightly decreased, and the thermal conductivity of PA/EP, SA/EP, and CA/SB was 0.0603, 0.0604, and 0.0624 W/m K, respectively. This result may be due to the interaction between EP and PA, leading to the scattering of heat carrier phonons (24,25). Another reason may be that the addition of organic acids increased the density of epoxy polymer chain, destroyed the continuity of epoxy polymer, and led to the change of its thermal conductivity (26,27). In all, the addition of organic acid coating could reduce the thermal conductivity of the samples, which made the SB have good thermal insulation performance and further improved the thermal behavior of SB.

Table 1: TGA data and thermodynamic parameters of the SB-based capsules

	T_0^{a} (°C)	T_f^{b} (°C)	L^{c} (%)	$T_0^{a'}$ (°C)	T_p^{d} (°C)	$T_f^{b'}$ (°C)	ΔT^{e} (°C)
NaHCO$_3$	119	186	37	119	152	188	69
EP@SB	155	180	32	151	171	197	46
PA/EP@SB	178	202	28	173	186	201	28
SA/EP@SB	174	199	24	169	186	200	31
CA/EP@SB	165	193	30	165	185	205	38

[a, a'] T_0: initial decomposition temperature. [b, b'] T_f: end thermal decomposition temperature. [c] L: weight loss of various SB-based capsules and pure SB. [d] T_p: peak endothermic temperature. [e] ΔT: thermal decomposition temperature range. $\Delta T = T_f - T_0$.
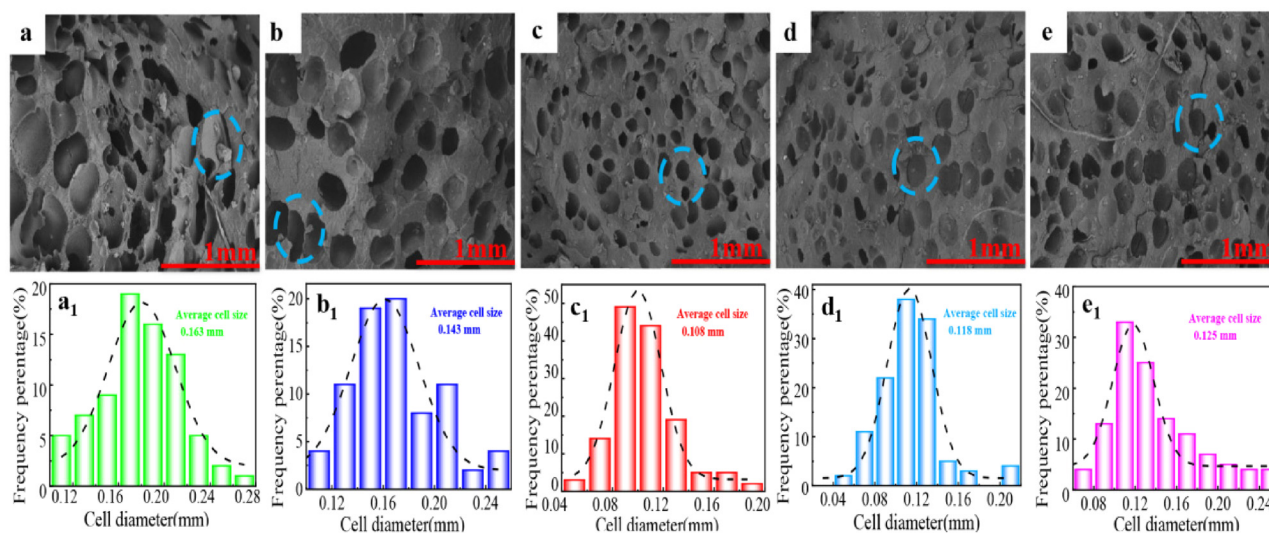
Figure 4: Cell structure (a–e) and the cell size distribution (a$_1$–e$_1$) of the PP foaming composites. (a) PP@SB, (b) PP/EP@SB, (c) PP/PA/EP@SB, (d) PP/SA/EP@SB, (e) PP/CA/EP@SB.

3.3 Foaming behavior and cell morphology

The good thermal insulation performance of the SB-based capsules encourages us to apply the modified SB as blowing agent to polyolefin foaming. The foaming process of SB in polyolefin was mainly composed of the formation of a stable gas-melt homogeneous system, cell nucleation, cell growth, and cell stability (28). Firstly,

to observe the foaming behavior of the SB-based capsules in PP, SEM was conducted. The average cell diameter and cell density were presented in Figures 4 and 5a and b. Figure 4a$_1$ showed the phenomenon of cell merging and collapse, and the cells were large and few. The cell diameter was 163 μm and the cell density was 0.872×10^5 cells/cm^3. This may be due to the rapid decomposition of SB, which could not be enriched in
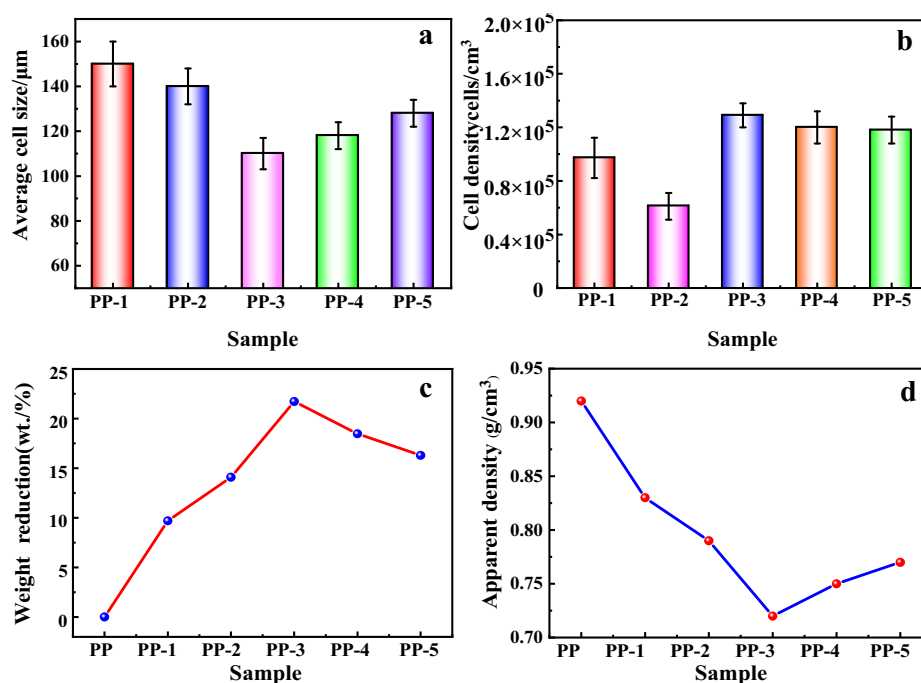

Figure 5: Cell parameters of the foamed PP composites: (a) average cell size, (b) cell density, (c) weight reduction, (d) apparent density.

PP polymer. In contrast, the cell size shown in Figure 4b$_1$ was relatively small, and the cell diameter and cell density were 142 μm and 0.961×10^5 cells/cm^3, respectively. Compared with Figure 4a$_1$, the cell density shown in Figure 4b$_1$ was more regular, which may be due to the increase of thermal stability and foaming temperature of SB@EP (29). Besides, the melting strength of the polymer matrix was enhanced by EP, and MMT and EP had a heterogeneous nucleation effect, resulting in the decrease of cell size and increase of cell density (30,31). The presence of less-foamed stage in Figure 4a$_1$ and b$_1$ was possibly due to the lower initial decomposition temperature of EP@SB and pure SB compared with the melting temperature of PP, resulting in the bubbles nucleation in the cell during cell formation (32–34). In other words, SB had already decomposed gas before some PP had not completely melted. In addition, with the introduction of organic acids in EP@SB, the cell density and cell size in samples of PP/SA/EP@SB and PP/CA/EP@SB shown in Figure 4d and e were 1.20×10^5 cells/cm^3, 1.18×10^5 cells/cm^3 and 118 μm, 125 μm in diameter, respectively. Notably, in the case of PA modifier, it can be clearly shown in Figure 4c$_1$ that there were many regular, uniform, and small cells in PP, and the cell density and cell size were 1.31×10^5 cells/cm^3 and 108 μm in diameter, respectively. This result was better than the reported melting modification method, as shown in Figure A4. Compared with Figure 4a$_1$, the average cell diameter in Figure 4c$_1$ reduced from 163 to 108 μm; the cells density increased from 0.872×10^5 to 1.31×10^5 cells/cm^3. Based on the above data analysis, it could be concluded that under the same amount of foaming agent, the foaming effect of organic acid-modified sodium bicarbonate in PP was superior than that of epoxy modified, and the long alkyl chain grafting improved the dispersibility of the CO$_2$ adduct in PP and favored a homogeneous release of CO$_2$ to blow PP during the exothermic foaming process (35).

As presented in Figure 5c, the weight of PP foaming products was reduced after foaming injection molding, and the weight reduction rates of PP/SB, PP/EP@SB, PP/PA/EP@SB, PP/SA/EP@SB, and PP/CA/EP@SB were 9.7, 14.1, 21.73, 18.47, and 16.30 wt%, respectively. In contrast, PP/PA/EP@SB exhibited the highest weight loss rate than others, indicating that PP/PA/EP@SB had the best foaming effect and the highest gas production, which may be due to the excellent compatibility of PP/PA/EP@SB in the PP foaming system, and its foaming temperature was closed to the melting temperature of PP. The apparent density of these PP foaming samples was also measured, as shown in Figure 5d. It could be seen that the apparent density of these PP materials was significantly decreased after foaming, and the apparent density of PP products using pure SB as foaming agent was the lowest. It was considered that the coating on SB improved the thermal properties of SB and further improved the foaming behavior of SB. Notably, the foamed PP samples prepared by blowing agents of PP/PA/EP@SB presented the lowest apparent density of 0.72 g/cm^3. This is because the interaction between EP and organic acid, which improved the performance of the coating, thereby further improved the thermal performance of SB, in turn affecting the foaming behavior of SB in PP. These data indicated that in the PP foaming system, by coating the foaming agent of SB with polymer or increasing the strength of the SB coating compound, the early decomposition of SB in PP can be restricted to achieve better foaming performance. This study not only conformed to the concept of environmentally friendly materials, but also provided direction guidance for the development of PP foaming products.

4 Conclusion

In summary, the green environmental SB foaming agent was modified by epoxy resin and some different organic acids. The modification of SB and its effect on foaming behavior of PP were investigated. After the modification, the decomposition temperature and decomposition temperature ranges of SB were significantly improved. In particular, compared with the pure SB, the decomposition temperature of PA/EP@SB composite increased from 119°C to 179°C, increased by nearly 50°C, and the decomposition temperature range was 41°C and 23°C lower than that of pure SB and EP@SB, respectively. Meanwhile, the foaming quality of PP was also significantly improved, and the cells were more uniform with smaller cells size and higher cells density compared to unmodified SB in PP. The results mainly ascribed to the addition of shells with EP and organic acids, which improved the thermal properties of SB, as well as enhanced the melt strength of PP. This study highlights that increasing the strength of the shell can enhance the decomposition temperature of SB and improve its foaming behavior in PP.

References

(1) Sukkaneewat B, Sridaeng D, Chantarasiri N. Fully water-blown polyisocyanurate- polyurethane foams with improved mechanical properties prepared from aqueous solution of gelling/blowing and trimerization catalysts. E-Polymers. 2016;19(1):277–89. doi: 10.1515/epoly-2019-0028.

(2) Liu L, Lv R. Synthesis of a DOPO-triazine additive and its flame-retardant effect in rigid polyurethane foam. E-Polymers. 2019;19(1):235–43. doi: 10.1515/epoly-2019-0024.

(3) Bayat H, Fasihi M, Zare Y, Rhee KY. An experimental study on one-step and two-step foaming of natural rubber/silica nanocomposites. Nanotechnol Rev. 2020;9(1):427–35. doi: 10.1515/ntrev-2020-0032.

(4) Charoeythornkhajhornchai P, Samthong C, Boonkerd K, Somwangthanaroj A. Effect of azodicarbonamide on microstructure, cure kinetics and physical properties of natural rubber foam. J Cell Plast. 2016;53:1–17. doi: 10.1177/0021955X16652101.

(5) Zeng GS, Lin RZ, Meng C, Zhai JP. The effect of the mixed foaming agent of azodicarbonamide and zinc oxide on the properties of foamed starch-based composite strengthened by plant-fibe. J Funct Mater. 2012;43(6):708–11. doi: 10.1364/JOSA.68.000480.

(6) Hussein MS, Leng TP, Rahmat AR, Zainuddin F, Keat YC. The influence of sodium bicarbonate loading as blowing agent on the properties of epoxy foam. Solid State Phenom. 2018;280:270–6. doi: 10.4028/www.scientific.net/SSP.280.270.

(7) Yao SJ, Zhou ZF, Ye F, Tian Z, Wang SM. Modifying sodium bicarbonate for foaming polymers. Adv Mater Res. 2014;940:59–62. doi: 10.4028/www.scientific.net/AMR.940.59.

(8) Petchwattana N, Covavisaruch S. Influences of modified chemical blowing agents on foaming of wood plastic composites prepared from poly(Vinyl Chloride) and rice hull. Adv Mate

Res. 2011;307:869–73. doi: 10.4028/www.scientific.net/AMR.306-307.869.

(9) Cao XW, Zhang Y, Wei W, Wu PJ. Thermal analysis of modified sodium bicarbonate. Chem Ind Eng Prog. 2012;31(10):2176–82. doi: 10.16085/j.issn.100-6613.2012.10.018.

(10) Contreras V, Maturana FJ, Jesús P, Núez KC, Pastor JM. Optimization of injection parameters to obtain selected properties on foamed PP with hollow glass microspheres and thermally expandable microspheres using Taguchi method. J Cell Plast. 2020;1–15. doi: 10.1177/0021955X20943097.

(11) Liang Y, Liu LZ, Zhang WL, Weng L, Hu DS, Li CY. Preparation and electrical properties of 4-acetoxystyrene grafted polypropylene for HVDC cable insulation. J Mater Sci-Mater El. 2020;31(5):3890–8. doi: 10.1007/s10854-020-02934-6.

(12) Tian B, Li ZG, Li JF, Yao G, Dong W, Liu YG, et al. The effects of rubber nanoparticles with different polarities on thermal properties and foaming performance of polypropylene blends. RSC Adv. 2020;10(52):31355–62. doi: 10.1039/D0RA04486E.

(13) Zhang Z, Li JS, Wang ZY, Long SY, Jiang SJ, Liu GL, et al. Preparation and performance characterization of a novel high-performance epoxy resin modified reactive liquid asphalt. Constr Build Mater. 2020;263:120113. doi: 10.1016/j.conbuildmat.2020.120113.

(14) Campuzano JF, Lopez ID. Study of the effect of dicumyl peroxide on morphological and physical properties of foam injection molded poly(lactic acid)/poly(butylene succinate) blends. Express Polym Lett. 2020;14(7):673–84. doi: 10.3144/expresspolymlett.2020.55.

(15) Gong W, Pei XL, Yin XG, Ban D, Fu H, He L. Synthesis of high-temperature thermally expandable microcapsules and their effects on foaming quality and surface quality of foamed ABS materials. E-Polymers. 2020;20:519–27. doi: 10.1515/epoly-2020-0021.

(16) Parsaee S, Mirabedini SM, Farnood R, Alizadegan F. Development of self aling coatings based on urea-formaldehyde/polyurethane microcapsules containing epoxy resin. J Appl Polym Sci. 2020;137(41):49663–15. doi: 10.1002/app.49663.

(17) Gyawali D, Nair P, Zhang Y, Tran RT, Chi Z, Samchukov M, et al. Citric acid-derived in situ crosslinkable biodegradable polymers for cell delivery. Biomaterials. 2010;31(34):9092–9105. doi: 10.1016/j.biomaterials.2010.08.022.

(18) Latibari ST, Mehrali M, Afifi ABM, Mahlia TMI, Akhiani AR, Metselaar HSC. Facile synthesis and thermal performances of stearic acid/titania core/shell nanocapsules by sol–gel method. Energy. 2015;85(1):1–10. doi: 10.1016/j.energy.2015.04.008.

(19) Liu J, Sun ZN, Wang F, Zhu D, Su H. Facile solvent-Free preparation of biobased rigid polyurethane foam from raw citric acid fermentation waste. Ind Eng Chem Res. 2020;59(22):10308–14. doi: 10.1021/acs.iecr.0c00946.

(20) Dai ZH, Han JR, Gao Y, Xu J, He J, Guo BH. Increased dielectric permittivity of poly(vinylidene fluoride-co-chlorotrifluoroethylene) nanocomposites by coating $BaTiO_3$ with functional groups owning high bond dipole moment. Colloid Surface A. 2017;592(20):560–70. doi: 10.1016/j.colsurfa.2017.05.065.

(21) Huo R, Zhang ZY, Athir N, Fan YH. Designing high thermal conductivity of cross-linked epoxy resin via molecular

dynamics simulations. Phys Chem Chem Phys. 2020;22:19735–45. doi: 10.1039/D0CP02819C.

(22) Maguire JM, Simacek P, Advani SG, Brádaigh CMÓ. Novel epoxy powder for manufacturing thick-section composite parts under vacuum-bag-only conditions. Part I: Through-thickness process modelling. Compos Part A-Appl S. 2020;136:105969. doi: 10.1016/j.compositesa.2020.105969.

(23) Ma IAW, Ammar SH, Bashir S, Selvaraj M, Assiri MA. Preparation of hybrid chitosan/silica composites via iono-tropic gelation and its electrochemical impedance studies. Prog Org Coat. 2020;145:105679. doi: 10.1016/j.porgcoat.2020.105679.

(24) Wang J, Xie H, Zhong X, Yang L. Increasing the thermal conductivity of palmitic acid by the addition of carbon nanotubes. Carbon. 2010;48(14):3979–86. doi: 10.1016/j.carbon.2010.06.044.

(25) Zhao J, Zhao Q, Wang C, Guo B, Park CB, Wang G. High thermal insulation and compressive strength polypropylene foams fabricated by high-pressure foam injection molding and mold opening of nano-fibrillar composites. Mater Design. 2017;131:1–11. doi: 10.1016/j.matdes.2017.05.093.

(26) Yang Z, Li J, Luan X, Song S. Effects of acid leaching and organic intercalation on the thermophysical properties of paraffin/expanded vermiculite composite phase change materials. Appl Clay Sci. 2020;196(5):105754. doi: 10.1016/j.clay.2020.105754.

(27) Zhang DL, Liu SN, Cai HW, Feng QK, Dang ZM. Enhanced thermal conductivity and dielectric properties in electrostatic self-assembly 3D pBN@nCNTs fillers loaded in epoxy resin composites. J Materiomics. 2020;6(4):751–9. doi: 10.1016/j.jmat.2020.06.013.

(28) Vadas D, Igricz T, Sarazin J, Bourbigot S, Marosi G, Bocz K. Flame retardancy of microcellular poly(lactic acid) foams prepared by supercritical CO₂-assisted extrusion. Polym Degrad Stabil. 2018;153:100–8. doi: 10.1016/j.polymdegradstab.2018.04.021.

(29) Zhang T, Jiang B, Huang Y. Combined use of methacrylate/epoxy functionalized silanes for tuning of hyperbranched polysiloxane structure. Mater Chem Phys. 2020;254:123525. doi: 10.1016/j.matchemphys.2020.123525.

(30) Li Y, Tian H, Jia Q, Niu P, Xiang A, Liu D, et al. Development of polyvinyl alcohol/intercalated MMT composite foams fabricated by melt extrusion. J Appl Polym Sci. 2015;132(43):42706–7. doi: 10.1002/app.42706.

(31) Wu S, He L, Zhang C, Gong W, Jiang T, Zhang X. Methodology for describing characteristic foam parameters during chemical foaming of low-density polyethylene. Mater Res Express. 2018;6(2):1–9. doi: 10.1088/2053-1591/aaec2d.

(32) Shaayegan V, Wang G, Park CB. Study of the bubble nucleation and growth mechanisms in high-pressure foam injection molding through in-situ visualization. Eur Polym J. 2015;76:2–13. doi: 10.1016/j.eurpolymj.2015.11.021.

(33) Zhu B, Zha W, Yang J, Zhang C, Lee LJ. Layered-silicate based polystyrene nanocomposite microcellular foam using supercritical carbon dioxide as blowing agent. Polymer. 2010;51(10):2177–84. doi: 10.1016/j.polymer.2010.03.026.

(34) Radhakrishna G, Dugad R, Gandhi A, Mohanty S, Nayak SK. Morphological evaluation of ultra low-density poly (methyl methacrylate) microcellular plastic developed through cyclic foaming technique. Int J Mater Eng Innov. 2019;10(4):310–32. doi: 10.1504/IJMATEI.2019.103611.

(35) Long Y, Sun F, Liu C, Huang D, Xie X. Climate-friendly poly-urethane blowing agent based on a carbon dioxide adduct from palmitic acid grafted polyethyleneimine. J Appl Polym Sci. 2016;133(35):43874–8. doi: 10.1002/app.43874.
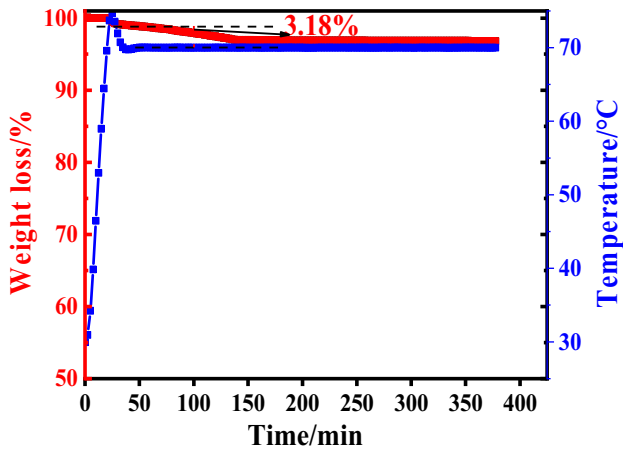
Appendix

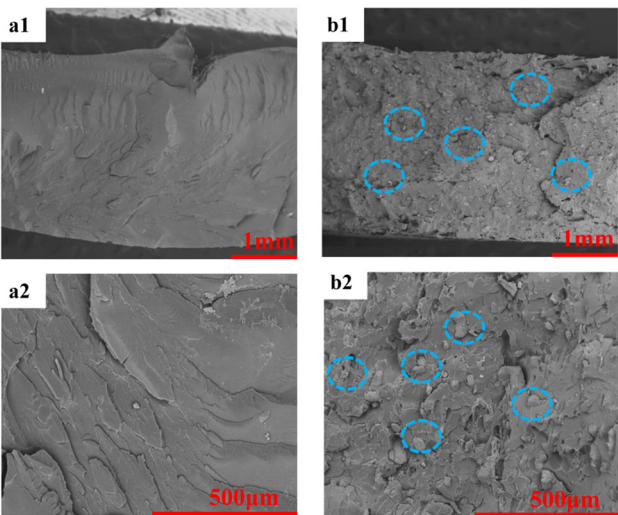**Figure A1:** Infrared curve of EP@SB before and after washing for 3 h.

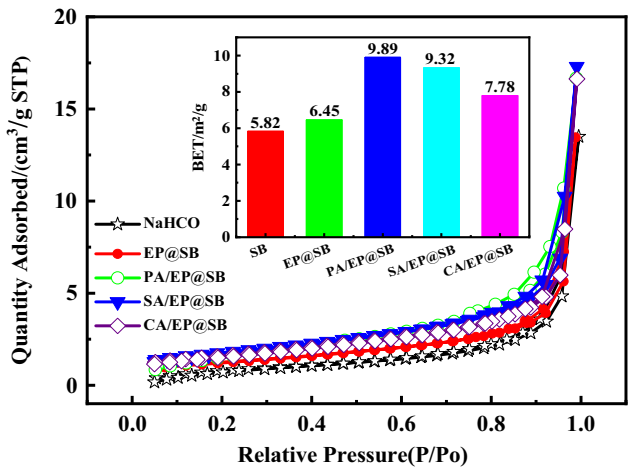**Figure A2:** SEM image of LDPE/(EP@SB) composite material.

Figure A3: Nitrogen adsorption isotherm of sodium bicarbonate of modification before and after modifying.
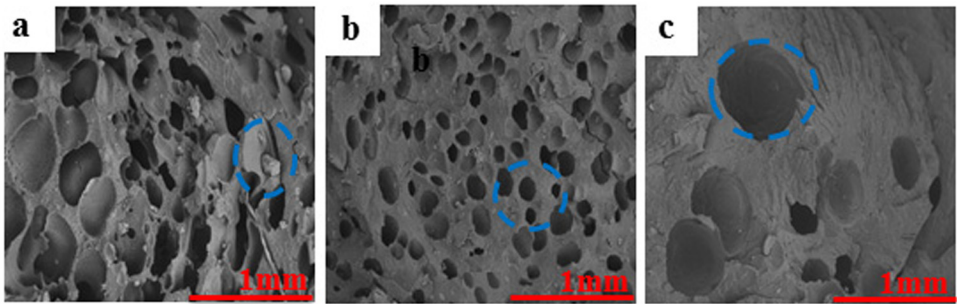

Figure A4: Cells structure of PP/MMT foams composites and cells size distribution: (a) PP/SB, (b)PP/PA/EP@SB, (c) PP/PA/EP@SB.